Fusion Engineering and Design 218 (2025) 115243

Contents lists available at ScienceDirect

Fusion Engineering and Design

journal homepage: www.elsevier.com/locate/fusengdes

Exploratory thermal and fluid-dynamic assessment of a pin of the Helium cooled pebble bed breeding blanket concept with a modular pin monoblock design for the EU DEMO nuclear fusion reactor

A. Gioè [a,*], F.A. Hernández [b], G. Bongiovì [a], A. Quartararo [a], E. Vallone [a], G. Agnello [a], G.A. Spagnuolo [c], S. d'Amico [c], P. Chiovaro [a], P.A. Di Maio [a]

[a] Dipartimento di Ingegneria, Università di Palermo, Viale delle Scienze, Ed. 6 90128, Palermo, Italia
[b] Institut für Neutronenphysik und Reaktortechnik (INR), Karlsruher Institut für Technologie (KIT), Eggenstein-Leopoldshafen 76344, Deutschland
[c] Fusion Technology Department – Programme Management Unit, EUROfusion Consortium, Boltzmannstraße 2 85748, Garching, Deutschland

ARTICLE INFO

Keywords:
DEMO
HCPB Bb
Thermofluid-dynamics
HCPB monoblock
CFD

ABSTRACT

The Helium-Cooled Pebble-Bed (HCPB) Breeding Blanket (BB) concept is one of the two candidates eligible for the driver blanket for the EU-DEMO nuclear fusion reactor. It foresees gaseous helium at high pressure as a coolant and tritium carrier, and solid tritium breeder and neutron multiplier. In order to overcome the potential showstoppers that emerged during its pre-conceptual design phase, alternative HCPB BB variants are under consideration in the frame of the DEMO studies. Among them, the concept envisaging a modular pin monoblock presents the advantages of having all the functional materials contained in a pin structure and of avoiding the need for a first wall, remarkably simplifying manufacturing. Hence, in this work, a campaign of thermofluid-dynamic scoping analyses aimed at assessing the performances of this novel BB concept is presented. To this scope, different geometric layouts have been assessed under a wide range of loading conditions and evaluating the sensitivity to key parameters, through cost-effective 2D CFD models. As an outcome, two promising geometric configurations ensuring both temperatures in line with the design requirements and an acceptable pressure drop have been found to be further assessed from the structural standpoint in a second phase of the activity.

1. Introduction

The construction of the EU-DEMO nuclear fusion reactor is envisaged by 2050 by the European research roadmap to the realisation of fusion Energy [1]. At the end of the DEMO Pre-Conceptual Design (PCD) phase, two Breeding Blanket (BB) concepts emerged as candidates for the driver blanket [2]: the Water-Cooled Lithium-Lead (WCLL) and the Helium-Cooled Pebble-Bed (HCPB). Currently, the DEMO Central Team (DCT) is investigating alternative configurations of the baseline WCLL [3] and HCPB [4] BB concepts, aiming to address the risks identified at the end of the PCD phase or to explore "high-risk, high-reward" designs [5,6].

Specifically, the HCPB BB concept foresees gaseous helium at 8 MPa as coolant and a further helium flow (with 100 Pa H2 to promote isotopic exchange) as tritium carrier and solid materials in the form of solid blocks and/or pebble beds as tritium breeder and neutron multiplier. An innovative HCPB BB concept based on a pin monoblock design, where all the BB functional materials (i.e., breeder and neutron multiplier) are contained within the fuel-breeder pins, is currently under study and is the subject of the present paper.

One of the major risks of the reference HCPB BB design is the possible loss of structural integrity of the prismatic $Be_{12}Ti$ multiplier blocks, which are placed around the pressure tubes, thus filling the volume among the fuel pins [7]. These blocks are not bonded to the pressure tubes, therefore the heat transfer happens through the minimum gas gap in between both. In the event of cracking, chunks of the multiplier may be detached and have insufficient cooling that may lead to unpredictable temperatures in the fragmented parts. Placing the $Be_{12}Ti$ or any other neutron multiplier also inside the fuel pins would create a modular pin design, where the pin modules are produced in series separately in a controlled area.

Moreover, the manufacturing of the pin concept is complex. Welding

* Corresponding author.
E-mail address: alberto.gioe@unipa.it (A. Gioè).

https://doi.org/10.1016/j.fusengdes.2025.115243
Received 17 January 2025; Received in revised form 29 April 2025; Accepted 30 May 2025
Available online 2 June 2025

each pressure tube to the First Wall (FW) requires methods that are currently not mature and, even when maturated, it would require joining ≈80,000 pressure tubes to the FW, representing a challenge in terms of time, cost and risks. The fabrication of an FW as a single part (or in a very limited number of parts, e.g. 2 or 3) is still deemed to be very challenging and its feasibility for a DEMO size is still to be demonstrated. Finally, the assembly sequence of the HCPB BB may be problematic due to the exposed presence of $Be_{12}Ti$ blocks [8].

These are the main reasons that brought to the introduction of the alternative HCPB BB design based on an innovative pin monoblock architecture (Fig. 1). This design is characterised by choices aiming at surmounting the above-mentioned critical issues. Indeed, the proposed new HCPB BB concept is characterized by the absence of a typical FW element/component and by modular fuel pins containing all the functional materials. Hence in this alternative HCPB BB concept, from now on indicated as "HCPB monoblock" for the sake of brevity, the new arrangement of breeder and multiplier avoids the occurrence of unpredictable temperature hotspots in neutron multiplier fragments, as the damaged block is cooled anyway, being located within the pin (namely within the actively cooled domain). Moreover, the absence of an FW strongly simplifies BB manufacturing.

In this context, a multi-physics scoping analysis, preparatory to a conceptual design of the HCPB monoblock BB concept, is presently ongoing at the University of Palermo in close cooperation with the DCT. In particular, the activity presented here regards the exploratory investigation of the steady-state fluid-dynamic and thermal behaviour of a pin of the HCPB monoblock BB concept, considering different geometric layouts and assessing the sensitivity to the variation of key parameters, such as surface roughness and cooling fluid temperature rise, under multiple loading scenarios. This investigation followed a theoretical-numerical approach based on the finite volume method and adopted the ANSYS FLUENT code. Due to the symmetry of the problem, a 2D model was employed, thus allowing to perform an extensive campaign of parametric analyses at a reduced computational cost. The scope of the work is to find out the best compromise between the pin's thermal behaviour (temperature should be limited in solid domains) and its fluid-dynamic performances (coolant speed and pressure drop are limited by DEMO design requirements), to assess the feasibility of the design from a thermal standpoint. In the following, models, assumptions, and primary findings are presented and discussed.

To this scope, the adopted geometric model is described in section 2 whereas the numerical model and the loading conditions adopted for the first campaign of parametric analysis are presented, together with the results, in section 3. In particular, this section details the setup (subsection 3.1), parameters (subsection 3.2) and results (subsection 3.3) of the baseline HCPB monoblock pin parametric analysis campaign. Based on the outcomes, the baseline geometric layout has been improved (section 4) and further assessed with detailed thermofluid-dynamic analysis, thoroughly described in section 5. Then, in section 6, studies on alternative configurations are presented and critically discussed. Finally, conclusions and follow-up are given in section 7.

2. Baseline HCPB monoblock pin geometry

In the baseline HCPB monoblock pin layout (Fig. 2) the breeder and the multiplier – constituted by Advanced Ceramic Breeder (ACB) pebble beds (Li_4SiO_4 + 35 %mol Li_2TiO_3) and $Be_{12}Ti$ blocks respectively – are arranged within a steel (ferritic-martensitic 9Cr-1WVTa steel, so called EUROFER97 and hereon referred to as "Eurofer" for the sake of readability) cladding, located in the actively cooled domain. The cooling helium enters the pin from the inlet manifold located in the back supporting structure, moves towards the Eurofer cap and spreads radially before moving backwards between the external Eurofer shell and the Eurofer outer sheet. Once the cooling helium reaches the Eurofer plug, it reverses its direction and flows between the Eurofer inner sheet and the Eurofer cladding, thus cooling the Breeding Zone (BZ) until it exits the pin domain to be collected in the outlet manifold. A thin layer of stagnant helium is interposed between the two Eurofer sheets in order to thermally decouple the cap – significantly affected by the heat flux acting on the tungsten plasma facing surface – from the BZ.

The stagnant helium layer and the flowing (cooling) helium form a continuous domain, as there is no physical separation between them. Specifically, the helium gap between the two Eurofer sheets is in direct communication with the main coolant flow in the zone of flow motion reversal, where no axial sealing is present between the sheets. On the opposite side of the gap, either an axial closure or an outlet leading to a confined region of stagnant helium located outside the pin domain is envisaged. Since both solutions ensure that the helium between the two Eurofer sheets remains effectively stagnant, further considerations are beyond the scopes of the pin's thermal and fluid-dynamic assessment.

3. Baseline HCPB monoblock pin parametric analysis campaign

The first step in the HCPB monoblock pin layout assessment was a parametric analysis focused on the reference pin geometry, considering multiple loading scenarios and different values of key parameters. A 2D axisymmetric model has been developed to perform the steady-state thermofluid-dynamic analyses with Ansys FLUENT at a reduced computation cost.

3.1. Thermofluid-dynamic analyses setup

The thermofluid-dynamic analysis campaign involved solid and fluid domains. The cooling helium has been modelled as an ideal gas with

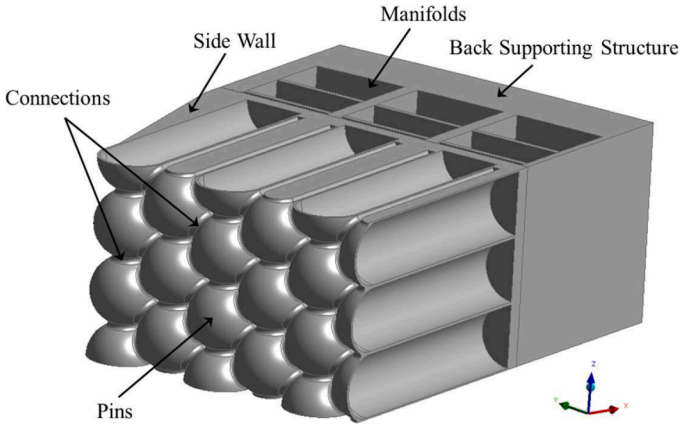

Fig. 1. 3D representation of the steel domains of the innovative pin monoblock architecture.

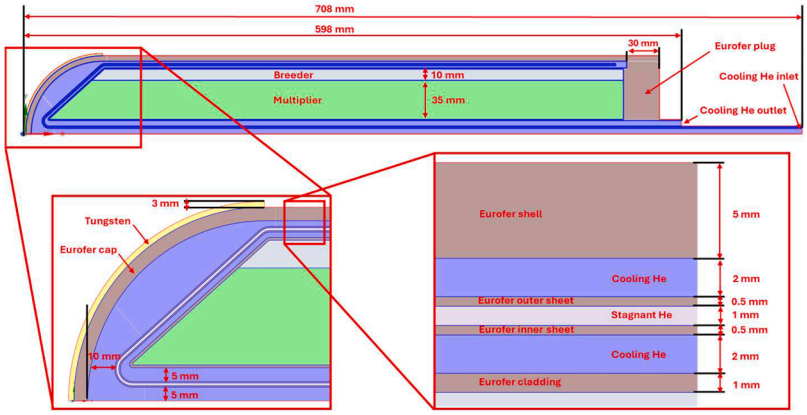

Fig. 2. 2D CAD model of the baseline HCPB monoblock pin layout (symmetric about the X-axis).

constant specific heat and temperature-dependent thermal conductivity and dynamic viscosity [9]. To reduce the computational burden, stagnant helium has been modelled as a solid with the same thermal conductivity as cooling helium. The solid domains (tungsten, structural Eurofer steel, ACB and $Be_{12}Ti$) have been modelled with temperature-dependent thermal conductivities [9]. Since the steady-state thermal field in solids does not depend on density and specific heat, constant values have been assigned to them. Two types of heat loads are considered:

- Nuclear Heating (NH), arising from the interactions of fusion neutrons and gammas with solid materials' nuclei, modelled as a volumetric heat source. Within tungsten, a uniform value of 25.9 W/cm^3 has been set [10]. Elsewhere, available data [11] relevant to the NHs acting on a similar all-in-pin HCPB BB concept have been mapped with decreasing exponential functions of the X coordinate fitted with the least square criterion (Fig. 3).
- Plasma surface loads acting on the tungsten plasma-facing surface, modelled as a not-uniform surface heat load varying accordingly to the loading scenario (see section 3.2).

The external surfaces not facing plasma have been considered adiabatic. In each analysis, the cooling helium Mass Flow Rate (MFR) has been tuned so to ensure the desired coolant temperature rise (parametrised, see 3.2.3) for every loading scenario. Table 1 summarizes the main analyses setup.

The domain discretization has been performed guaranteeing a minimum of three elements across the thickness of the thinnest regions, namely the Eurofer sheets, to ensure that heat diffusion phenomena are accurately captured. Moreover, the mesh has been refined in the jet impingement and fluid motion reversal (close to the Eurofer plug) zones where more complex flow features are expected. Discretization characteristics are summarized in Table 2.

Table 1
Summary of thermofluid-dynamic analyses setup.

Analysis Setting	Value
Analysis Type	Steady-state
Domain Features	2D axisymmetric
Fluid Inlet Temperature	300 °C
Inlet BC	MFR
Outlet BC	8 MPa total pressure
Turbulence Model	k-ω SST
Wall BCs	No-slip rough wall condition

Table 2
Summary of mesh main parameters.

Mesh Parameter	Value
Nodes/Elements	$6.6{\cdot}10^5/6.6{\cdot}10^5$
Elements Topology	Hybrid (Quad/Tria)
Inflation Layer Number	20
First Layer Thickness [μm]	2
Layers Growth Rate	1.3
Element size [mm]	0.5/0.25 in refined zones

3.2. *Parameters of the thermofluid-dynamic analysis campaign*

The considered parameters in the baseline HCPB monoblock pin layout scoping thermofluid-dynamic analyses concern the tungsten heat load, the surface roughness and the coolant temperature rise.

3.2.1. *Heat flux on tungsten plasma-facing surface*

The thermal effects of the electromagnetic radiation emitted by plasma are modelled as a surface heat load acting on the tungsten hemispherical plasma-facing surface. The imposed heat flux has a maximum value HF_0 at the tip ($r = 0$) and decreases down to 0 W/m^2 at the side ($r = R$, with $R = 72$ mm), according to Eq. (1). The parametric analyses considered five different HF_0 values, equally ranging from 0.3

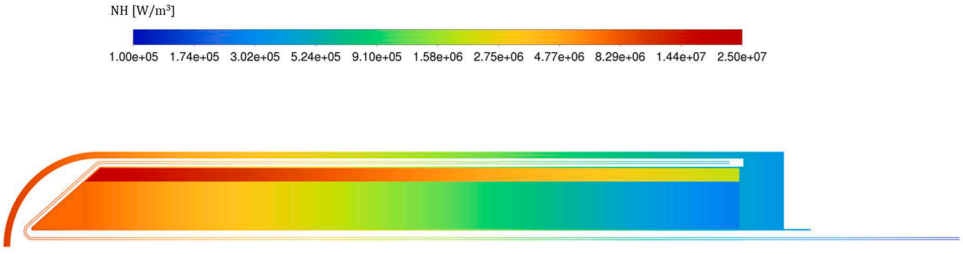

Fig. 3. Nuclear Heating applied to breeder, multiplier, and Eurofer domains.

MW/m^2 to 1.0 MW/m^2.

$$HF = HF_0 \cos\left(\sin^{-1}\left(\frac{r}{R}\right)\right) \quad (1)$$

3.2.2. Wall surface roughness

Certain coolant-wetted regions of the HCPB monoblock baseline pin layout supposedly present the manufacturing feasibility of surface finishing. A local increase in surface roughness locally enhances the solid-fluid heat transfer at the cost of worsened behaviour in terms of pressure drop. In the presented analyses, five different values of sand grain roughness have been considered on the coolant-wetted parts of the Eurofer cladding and of the Eurofer inner sheet (see Fig. 2), equally spaced from 20 μm to 100 μm. A constant value of 20 μm has been kept elsewhere.

3.2.3. Cooling helium temperature rise

Increasing the coolant temperature rise in steady-state conditions allows to work with lower MFRs and total pressure drops, thus reducing the required pumping power. Furthermore, higher coolant outlet temperatures result in a more efficient thermal-to-electric energy conversion. Nevertheless, increasing the coolant temperature rise, higher temperatures in the solid domains are expected, possibly jeopardizing the structural material integrity. Keeping the coolant inlet temperature fixed at 300 °C (Table 1), the helium outlet temperature has been changed so to consider five different values of coolant temperature rise, equally ranging from 220 °C to 300 °C.

3.3. Results of the parametric analysis campaign

The main outcomes of the parametric analysis campaign (section 3.3.1) and of the related grid independence analysis (section 3.3.2) are hereby presented and critically discussed.

3.3.1. Outcomes of the parametric analysis campaign

All the investigated cases present maximum Eurofer temperatures over the 550 °C DEMO design limit for parts with a structural function. Nevertheless, the collected data allowed a better understanding of the HCPB monoblock pin's overall thermal and fluid-dynamic performance (see Fig. 4 and Fig. 6 relevant to the pin reference working conditions, namely 0.3 MW/m^2 HF_0 and 220 °C coolant temperature rise). Moreover, the following trends emerge from the collected data:

- as visible in Fig. 5a, the overall temperature distribution in the tungsten, breeder, and multiplier domains poses no concerns (thanks to wide margins against their respective design limits of 1050 °C, 970 °C, and 1050 °C [12]), while multiple Eurofer domains are close to the 550 °C threshold, and the cladding is far beyond. Although the cladding is not considered to have a structural function in the pin and it only contains the functional material without sustaining a pressure difference, such high temperatures may still jeopardize the concept's reliability due to thermal stresses. This will be a matter of further structural studies. Other cladding materials (e.g. SiC) may be proposed, also in view of a better compatibility with the ceramic material and lower tritium permeation rates.
- as can be observed in Fig. 5b, increasing HF_0 produces a reduction in the maximum Eurofer temperature as it improves the thermal field in the hottest region of the Eurofer domain - located in the cladding - due to the increased MFR (required for a fixed coolant temperature rise). However, the cap maximum temperature increases, exceeding 550 °C for HF_0 values higher than 0.6 MW/m^2. As this hot spot is localized, further structural analyses are needed to evaluate if overcoming the temperature design limit does not represent an issue here;
- an increase of sand grain roughness on machined surfaces allows for a reduction of the maximum Eurofer temperature (up to 11 °C when it changes from 20 μm to 100 μm) as it enhances the heat exchange in the cladding. However, the effect of the roughness is not very significant, therefore a cost-benefit analysis should be done to evaluate if this temperature margin increase is worth the additional manufacturing complexity to increase the surface roughness in these inner surfaces;
- for each 1 °C increase in the coolant temperature rise, the maximum Eurofer temperature is increased by 1.4 °C;
- the total pressure drop exhibits a slight sensitivity to roughness and a pronounced dependence on the MFR, which can be deduced from the trend observed in Fig. 5b

The observed trends allowed to draw the following conclusions on the HCPB monoblock baseline pin design, which paved the way for the subsequent design optimization:

- it is necessary to enhance the fluid-solid heat exchange in the Eurofer cladding region;
- potentially, working configurations can be found with HF_0 values higher than 0.3 MW/m^2;
- surface finishing in critical surfaces helps in lowering the maximum Eurofer temperature;
- only a substantial design improvement may allow HCPB monoblock pin operation with coolant temperature rise higher than 220 °C;
- the total pressure drop is rather low, hence it is possible to explore solutions which improve the thermal field at the cost of a worsened fluid-dynamic behaviour.

Summarising, the parametric analysis campaign carried out on the baseline HCPB monoblock pin layout highlighted the necessity of updating the pin design to lower the temperatures achieved in the Eurofer domains, especially in the cladding region. Moreover, the low pressure drop allowed considering solutions where enhanced heat transfer is achieved with higher pressure losses.

3.3.2. Parametric analysis campaign - grid independence evaluation

To ensure that the results presented in section 3.3.1 are not affected by inadequate domain discretization, grid independence analysis has been performed. Considering the pin reference working conditions and a roughness value of 20 μm, it has been verified that minimal result variations occur when doubling the mesh element size twice. For the sake of

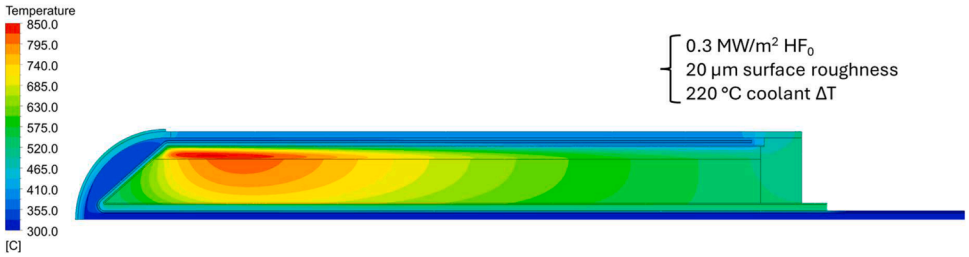

Fig. 4. Temperature field in solid and fluid domains.

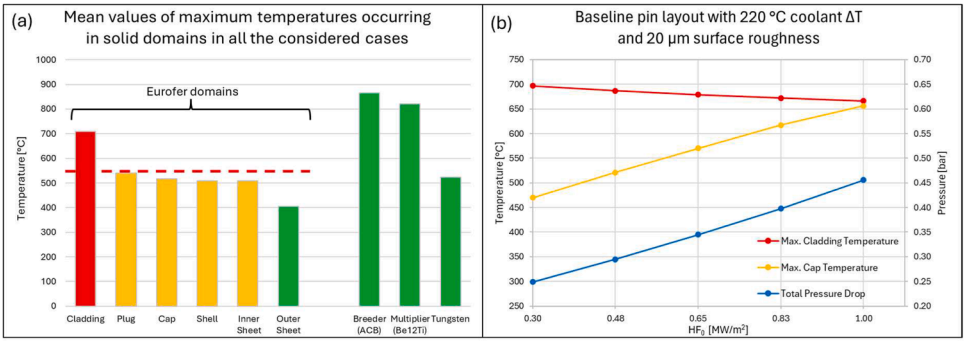

Fig. 5. Mean values of temperature peaks in the different structures (a) and baseline pin performance sensitivity on HF0 (b).

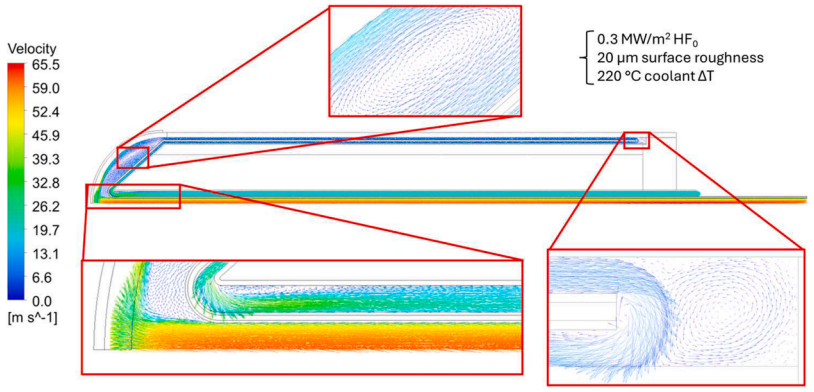

Fig. 6. Fluid velocity vector plot: details of vortices and fluid vein detachments.

brevity, solely the percentage differences of the evaluated total pressure drop are presented in Table 3.

4. HCPB monoblock pin layout updates

On the basis of the results reported above, two alternative pin layouts have been created. Since one cannot exclude a priori that the trends described in section 3.3.1 may vary upon pin design update, the same parameters (along with the relevant ranges) described in section 3.2 have been considered.

4.1. Geometry updates and analyses setup

In order to ensure higher flow speed and higher heat transfer coefficients in the cladding region, at the expense of an increased pressure drop, the height of the outlet annular channel has been reduced from 5 mm to 2 mm. Thus, two new geometric layouts have been created (Fig. 7):

- case 2, where the height reduction is performed by increasing the stagnant helium gap thickness;
- case 3, in which the height reduction is performed by increasing the multiplier volume.

Table 3
Grid independence analysis results.

Element size [mm]	Nodes/Elements	Percentage variation of evaluated total pressure drop
0.5/0.25 in refined zones	$6.6{\cdot}10^5/6.6{\cdot}10^5$	0.0 % (Reference)
1/0.5 in refined zones	$5.8{\cdot}10^5/5.8{\cdot}10^5$	−0.14 %
2/1 in refined zones	$5.5{\cdot}10^5/5.6{\cdot}10^5$	−0.54 %

4.2. Thermal and fluid-dynamic performance of alternative layouts

Averaging the collected data in all the considered scenarios, case 2 presents - 10 °C maximum Eurofer temperature and - 29 % total pressure drop with respect to case 3 (details in Fig. 8a). This can be explained considering that the increased multiplier volume of case 3 geometry results in higher deposited power, and that the cross-section of the outlet annular channel of case 3 layout is smaller compared to that of case 2 geometry, as it is located closer to the X symmetry axis. Due to this difference, attention is paid to the case 2 results and their comparison with the baseline. In both cases the Eurofer temperature always exceeds the 550 °C limit, but this happens only in the cladding, where this concern is lower. In any case, a remarkable improvement in the Eurofer thermal field has been achieved (Fig. 8b) at the cost of a worsened -yet acceptable- pressure drop.

It is worth noting that the non-monotonic trend in maximum Eurofer temperature for case 2 with increasing values of HF_0 is due to the fact that, at some point between 0.65 MW/m^2 and 0.83 MW/m^2 HF_0, the location of the highest Eurofer temperature shifts from the cladding to the cap. Hence, this trend arises from the strongly improved thermal behaviour that is achieved in the cladding upon design update. Moreover, a 21 °C decrease in the maximum Eurofer temperature is achieved when the roughness of machined surfaces changes from 20 to 100 μm. Hence, case 2 geometry appears to be more sensitive to surface finishing with respect to baseline, where the homologous quantity is 11 °C (see section 3.3.1). On these bases, the case 2 layout has been selected for more detailed investigations.

5. Detailed analysis of case 2 layout performance

Adopting the case 2 geometric layout, the possibility of extending the areas interested by surface finishing and increasing the roughness value beyond 100 μm was explored. In addition, the pressure drop distribution

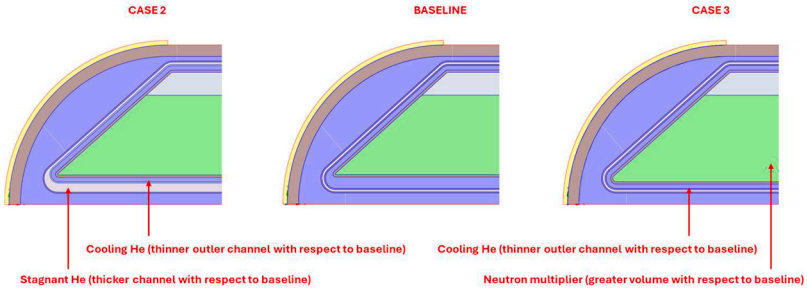

Fig. 7. Apical area of baseline geometry (middle) and the two alternative layouts (sides).

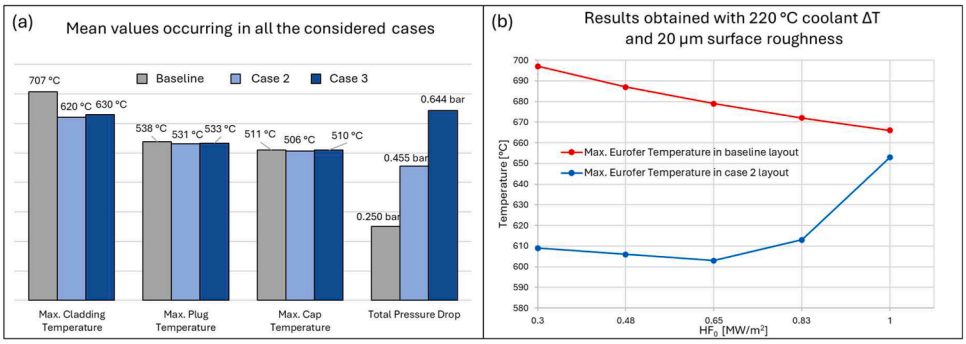

Fig. 8. Comparison of the performances of the three layouts (a), and case 2 VS baseline (b).

along the flow path was evaluated to gather information for further improvements.

5.1. Setup of analyses focused on case 2 layout

The further exploratory analyses carried out on the case 2 HCPB monoblock pin layout used the same parameter sets described in section 3.2 except for the roughness, since the surface finishing has been further extended to the cap hemispherical inner surface. Furthermore, on the machined surfaces roughness of 100 μm and 200 μm has been considered while 20 μm has been kept elsewhere. The analysis setup is that of Table 1. Nevertheless, due to the high degrees of surface machining, the Ansys Fluent High Roughness (Icing) model has been used, updating the mesh accordingly (see Table 4).

5.2. Results of the analyses focused on case 2 layout

The analyses focused on case 2 layout with high levels of surface roughness exhibited maximum Eurofer temperatures higher than 550 °C. Nevertheless, in some cases, the Eurofer thermal field is very close to the prescribed limit, as one can observe from the trends shown in Fig. 9a. In detail, comparing Fig. 9a and Fig. 5b, it can be deduced that the pin layout optimization has led to a maximum Eurofer temperature reduction of 132 °C for the HCPB monoblock pin under reference working conditions. Furthermore, the total pressure drop has further increased due to the roughness values assumed in more extended areas (Fig. 9b).

Table 4
Summary of high roughness analyses mesh main parameters.

Mesh Parameter	Value
Nodes/Elements	$8.8{\cdot}10^5/8.8{\cdot}10^5$
Elements Topology	Hybrid (Quad/Tria)
Inflation Layer Number	29
First Layer Thickness [μm]	0.2
Layers Growth Rate	1.3
Element size [mm]	0.5/0.25 in refined zones

Moreover, it has been found that, among the considered parameters, the pressure drop breakdown along the flow path (Table 5) is only sensitive to the roughness value on machined surfaces. Notably, in all the investigated cases, 94 % of the pressure drop occurred in solely three regions, namely the inlet tube, the cap, and the outlet channel. Hence, attention should be focused on the aforementioned regions for any future attempt to improve the HCPB monoblock pin fluid-dynamic behaviour.

6. Investigation on alternative layouts

The multiphysics scoping analysis conducted on the HCPB monoblock innovative BB design has allowed obtaining a preliminary design optimization, resulting in a 132 °C reduction in the maximum Eurofer temperature occurring in the pin under reference working conditions, with respect to the baseline configuration. Moreover, the collected data on the pressure drop breakdown along the flow path and on the pin behaviour upon variation of key parameters constitute a relevant asset for any further design optimization. On this basis, the investigation has been continued exploring alternative geometric layouts with quite remarkable differences with respect to the baseline configuration.

6.1. Alternative geometric layout

Since the obtained results in terms of maximum Eurofer temperatures are encouraging, two further layouts were conceived to improve the pin performance in terms of thermal field in the cap and in the cladding, and of pressure drop. They are hereon referred to as case 4 and case 5 layout.

6.1.1. Case 4 layout

The case 4 geometry is obtained starting from case 2 layout, by modifying the geometry in the cap region (namely the pin front region) as shown in Fig. 10. Here, the clearance for the cooling helium flow in the proximity of the Eurofer cap is 2 mm. This modification is aimed at investigating whether a more controlled helium flow in the cap region

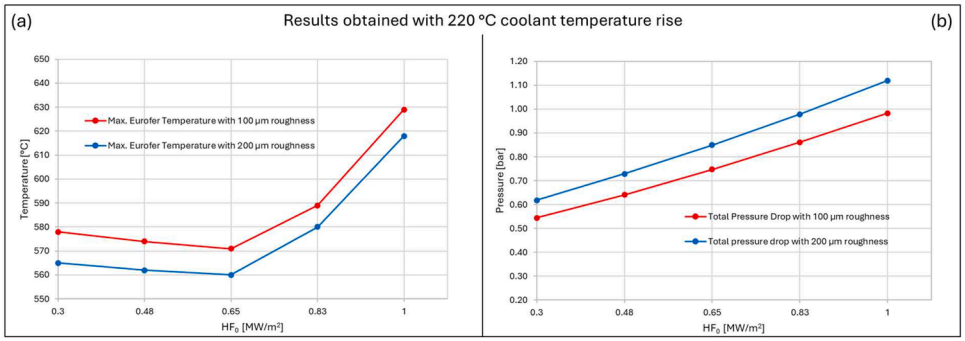

Fig. 9. Results of case 2 pin layout with different levels of roughness on machined surfaces.

Table 5
Pressure drop breakdown (fraction of the total pressure drop) in case 2 pin layout.

Roughness on machined surfaces [µm]	Fraction of total pressure drop [%]			
	Inlet tube	*Cap*	*Outlet Channel*	*Other regions*
20	31	16	47	6
100	26	14	54	6
200	23	11	60	6

enhances the heat transfer in this critical region.

6.1.2. Case 5 layout

The case 5 layout is rather different from the former ones, obtained starting from the case 2 layout by removing the metal sheets and the stagnant helium, and enlarging the breeder and multiplier by occupying the free space (see Fig. 11, comparing case 2 and case 5 layout). As visible in the figure, the case 5 layout foresees a "one way" cooling helium flow path from inlet to outlet in the pin domain. This geometry is meant to improve the thermal behaviour of the cladding by ensuring lower cooling helium temperatures in its proximity, and to lower the pressure drop by getting rid of the "outlet channel" contribution, which is the greatest in the case 2 layout (see Table 5).

6.2. Numerical modelling

The numerical modelling adopted for the investigation on the alternative case 4 and case 5 HCPB monoblock pin layouts is rather similar to that adopted for the in-depth analyses on case 2 geometry described before, hence this section briefly illustrates the differences between the two.

For the case 4 analysis, the same parameters and ranges described in section 5.1 have been used. As to case 5 geometry, due to the simplified geometry, the feasibility of surface machining has been assumed over all the coolant-wetted surfaces. Hence, in the parametric analyses focused on the case 5 layout, the roughness value has been uniformly set in all the coolant-wetted surfaces, and the same ranges of variation of section 5.1 have been used.

The same discretization settings of Table 4 have been used, which resulted in a mesh of $8.85{\cdot}10^5$ nodes and $8.84{\cdot}10^5$ elements for the case 4 layout, and of $3.61{\cdot}10^5$ nodes and $3.59{\cdot}10^5$ elements for the case 5 layout. The number of nodes and elements constituting the case 5 numerical model is significantly lower compared to the other models because of the reduction of the area of coolant-wetted surfaces, where mesh inflation is performed.

6.3. Results

Results obtained for case 4 and case 5 have been compared with the results of case 2 which presents the best performance among the analysed first three cases. The comparison is performed by averaging, for each layout, the results obtained for all the considered sets of parameters. Detailed comparisons have been performed but, for the sake of brevity, only the main trends that emerged are presented and discussed hereafter.

6.3.1. Case 4 layout

Compared to the case 2 layout, case 4 exhibits a reduction in the pressure drop that occurs in the jet zone, but at the cost of a substantial worsening of the cap thermal field. The overall performance of the two layouts has been compared by averaging the results obtained in the two geometries under the considered cases and making the difference of relevant quantities, as visible in Table 6.

It is worth noting that the case 4 layout presents a total pressure drop that is, on average, 2.10 % greater than that of case 2 layout. Nevertheless, this increase is lower than 5.30 %, which is the increase predicted by applying a quadratic model for pressure drop dependence on velocity, and extrapolating the value that would have been obtained in

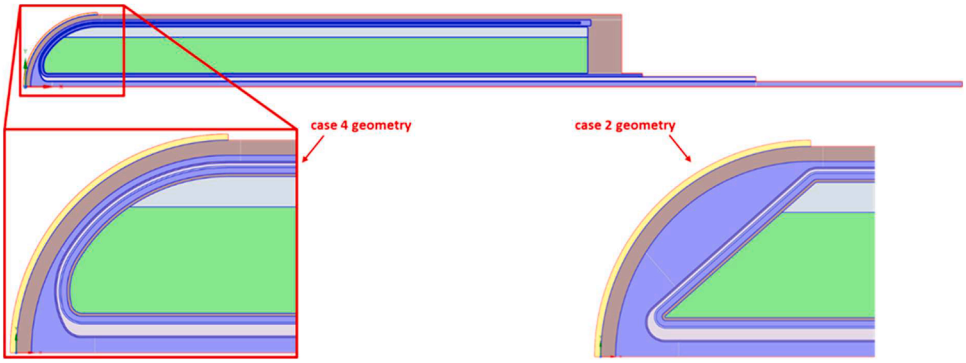

Fig. 10. Case 4 geometry and comparison with case 2 layout.

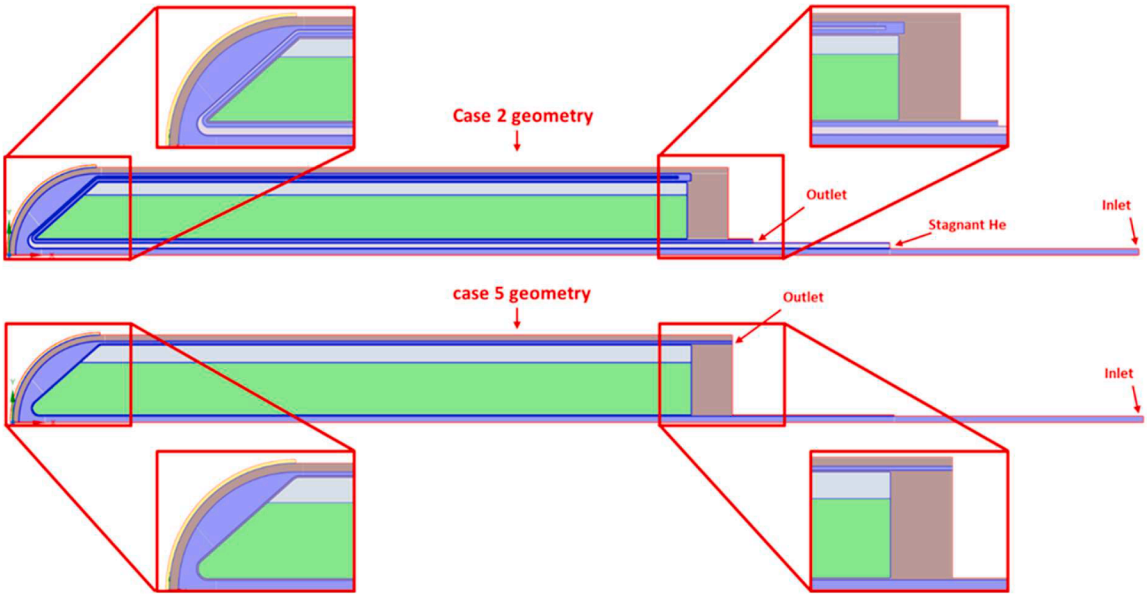

Fig. 11. Case 5 geometry and comparison with case 2 layout.

Table 6
Difference between average results obtained in case 4 and in case 2 layouts.

	Mass flow	V inlet	Δp tot	T_{max} cladding	T_{max} plug	T_{max} cap	T_{max} shell	T_{max} inner sheet	T_{max} outer sheet	T_{max} breeder	T_{max} multiplier	T_{max} tungsten
	[kg/s]	[m/s]	[%]	[°C]	[°C]	[°C]	[°C]	[°C]	[°C]	[°C]	[°C]	[°C]
Average deviation	8E-04	1.43	2.10 (vs. 5.30)	0.7	−0.4	53	0.5	0.2	−0.3	28	5	53

case 2 layout with the increased average inlet velocity occurring in case 4 layout (that is due to the increased MFR, consequence of greater breeder and multiplied volume and hence greater deposited power, which requires higher MFR for given coolant temperature rise). This trend is a consequence of the lower total pressure drop occurring in the cap region of the case 4 layout, whereas the remaining part of the geometry is equal in the two layouts. Moreover, observing Table 6 it can be noticed that the maximum Eurofer Cap temperatures are significantly higher in the case 4 layout compared to the case 2. This can be explained by observing Fig. 12: the jet impingement geometry of case 4 causes lower cooling helium velocities in the proximity of the Eurofer cap compared to case 2, which implies lower HTCs and, finally, higher temperatures within the cap.

6.3.2. *Case 5 layout*

The case 5 layout is the first investigated geometry showing

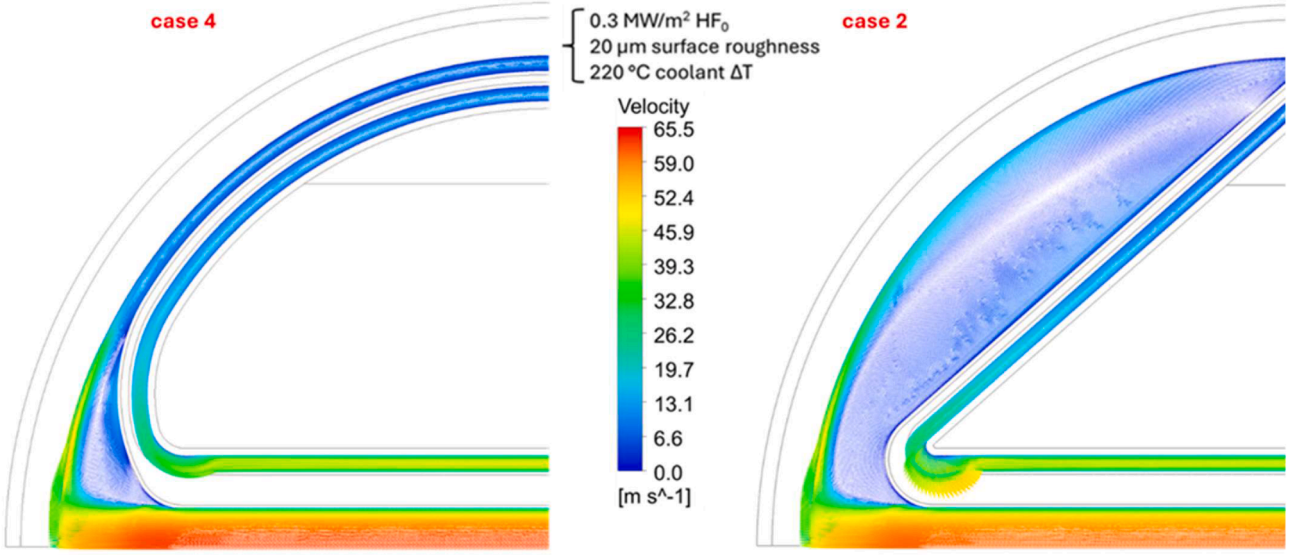

Fig. 12. Fluid velocity vector plot in jet impingement region of case 4 and case 2 layouts.

temperatures lower than 550 C° in all the Eurofer domains for at least one combination of parameters. Specifically, this occurs in two investigated cases: the case with $HF_0 = 0.30$ MW/m^2, Helium $\Delta T = 220$ °C and roughness of 100 μm and the case with $HF_0 = 0.30$ MW/m^2, Helium $\Delta T = 220$ °C and roughness of 200 μm. Compared to the case 2 layout, the case 5 layout exhibits a significant reduction of the total pressure drop and of the maximum cladding temperatures, but at the cost of a substantial worsening of the cap and shell thermal fields, which are key structural elements of the segment. The overall performance of the two layouts has been compared by averaging the results obtained in the two geometries under the considered cases and making the difference of relevant quantities, as visible in Table 7.

In the comparison of the results, it is worth pointing out that the increase in the breeder and multiplier volume results in $a + 17$ % in the total deposited power in this layout compared to the case 2 layout for $HF_0 = 0.3$ MW/m^2. Hence, the results shown correspond to significantly different flow velocities, as can be seen in Table 7. Despite that, the case 5 layout presents remarkably lower pressure drops than case 2, as it does not foresee the coolant flow in the small outlet channel of the case 2 layout, which is where the greatest pressure loss occurs in case 2 geometry (see Table 5). The total pressure drop of case 5 layout is, in most cases, between 0.3 bar (0.03 MPa) and 0.6 bar (0.06 MPa). The change in the cladding, cap, and shell thermal behaviour can be explained through the loss of thermal decoupling between the external Eurofer regions and the BZ, which was realized through the stagnant helium in the other designs.

7. Conclusion and follow-up

A multiphysics scoping analysis campaign has been conducted on the HCPB monoblock pin for a preliminary assessment and optimization of its thermal and fluid-dynamic behaviour, through 2D CFD analyses performed on Ansys Fluent.

First, an exploratory analysis campaign studied three different layouts under multiple thermal loading scenarios and considering the influence of key parameters such as roughness on certain surfaces and coolant temperature rise. This campaign allowed for a first pin characterization from the thermal and fluid-dynamic standpoints, and highlighted the presence of one preferable layout - namely the case 2 geometry - and the importance of the contribution of high values of roughness on lowering the maximum Eurofer temperatures.

Subsequently, in-depth parametric analyses have been carried out on the case 2 layout considering high values of roughness (up to 200 μm). These analyses showed that this pin design allows to keep maximum Eurofer temperatures below 610 °C in most of the considered cases and close to 550 °C in some working conditions. The pin's total pressure drop is rather sensitive to the considered case, but in these analyses it resulted to be between 0.5 bar (0.05 MPa) and 0.8 bar (0.08 MPa) in the majority of the cases.

Finally, two alternative layouts, conceived to improve the case 2 layout based on the trends that emerged from its detailed assessment, have been investigated. Among these, the case 5 layout presented Eurofer temperatures lower than 550 °C in two of the considered cases and a pressure drop rather lower compared to that of the case 2 layout, between 0.3 bar (0.03 MPa) and 0.6 bar (0.06 MPa) in most of the cases.

In conclusion, the preliminary design optimization allowed to find two pin layouts, namely the case 2 and case 5 geometry, that exhibit rather promising thermal and fluid-dynamic behaviour. Hence, the follow-up of this work will foresee the preliminary thermomechanical assessment of such promising configurations.

In case of positive outcomes of the structural assessment, it may be worthwhile to analyse additional layouts to further improve the thermofluid dynamic behaviour of the concept in light of the results presented in this work. For instance, one possible update of the case 2 layout may foresee an increased diameter of the inlet tube (obtained with a reduction in the thickness of the stagnant helium layer) which would result in lower coolant velocities in that region and, potentially, in a reduction of the total pressure drop to a similar level as the baseline case. However, the investigation on the case 4 layout highlighted the strong impact of flow velocities in the front region on the cap thermal behaviour, hence the new diameter may be found performing a trade-off between a lower total pressure drop and a higher maximum cap temperature, or, alternatively, the increase in the diameter may be accompanied by a reshaping of the jet impingement region aimed at producing a localized increase in flow velocities in the cap zone. On the other hand, a better solution may also be pursued by updating the case 5 layout, which benefits from significantly higher breeder and multiplier volumes (with positive consequences on the tritium breeding ratio) and from the simplest pin design among the considered ones (generally leading to higher concept reliability and less demanding manufacturing). In this case, exploiting the comparatively low total pressure drop, it may be considered to reduce the inlet tube diameter and the area of the outlet annular section in the quest for a trade-off between higher total pressure drop and lower cap and shell maximum temperatures. Moreover, also in this case, reshaping the jet impingement region may be considered in order to locally increase coolant velocities in the cap zone, and the optimal solution may emerge as a combination of the proposed layout updates.

Ultimately, in advanced design stages, a 3D CFD model may be implemented to provide a more detailed thermal and fluid-dynamic assessment of the optimized pin layout which would emerge following the study of the BB concept structural behaviour.

CRediT authorship contribution statement

A. Gioè: Writing – review & editing, Writing – original draft, Methodology, Investigation, Formal analysis, Data curation, Conceptualization. **F.A. Hernández:** Writing – review & editing, Supervision, Methodology, Conceptualization. **G. Bongiovì:** Writing – review & editing, Writing – original draft, Methodology, Investigation, Formal analysis, Data curation, Conceptualization. **A. Quartararo:** Writing – review & editing, Writing – original draft, Methodology, Investigation, Formal analysis, Data curation, Conceptualization. **E. Vallone:** Writing – review & editing, Writing – original draft, Methodology, Investigation, Formal analysis, Data curation, Conceptualization. **G. Agnello:** Writing – review & editing, Writing – original draft, Methodology, Investigation, Formal analysis, Data curation, Conceptualization. **G.A. Spagnuolo:** Writing – review & editing, Supervision, Methodology, Conceptualization. **S. d'Amico:** Writing – review & editing, Supervision, Methodology, Conceptualization. **P. Chiovaro:** Writing – review & editing, Methodology, Investigation, Formal analysis, Data curation, Conceptualization. **P.A. Di Maio:** Writing – review & editing, Methodology, Investigation, Formal analysis, Data curation, Conceptualization.

Declaration of competing interest

The authors declare that they have no known competing financial interests or personal relationships that could have appeared to influence

Table 7
Difference between average results obtained in case 5 and in case 2 layouts.

	Mass flow	V inlet	Δp tot	T_{max} cladding	T_{max} plug	T_{max} cap	T_{max} shell	T_{max} breeder	T_{max} multiplier	T_{max} tungsten
	[kg/s]	[m/s]	[%]	[°C]	[°C]	[°C]	[°C]	[°C]	[°C]	[°C]
Average deviation	4.3E-03	8.22	−25	−33	−4	75	40	189	84	75

the work reported in this paper.

Acknowledgments

This work has been carried out within the framework of the EUROfusion Consortium, funded by the European Union via the Euratom Research and Training Programme (Grant Agreement No. 101052200 — EUROfusion). Views and opinions expressed are however those of the author(s) only and do not necessarily reflect those of the European Union or the European Commission. Neither the European Union nor the European Commission can be held responsible for them.

Data availability

Data will be made available on request.

References

[1] T. Donné, et al., European Research Roadmap to the Realisation of Fusion Energy, EUROfusion, Munich, Germany, 2018. ISBN 978-3-00-061152-0.
[2] F.A. Hernández, et al., Advancements in Designing the DEMO driver blanket system at the EU DEMO Pre-conceptual design phase: overview, challenges and opportunities, J. Nucl. Eng. 4 (3) (2023) 565–601, https://doi.org/10.3390/jne4030037.
[3] P. Arena, et al., The DEMO water-cooled lead–lithium breeding blanket: design status at the end of the pre-conceptual design phase, Appl. Sci. 11 (24) (2021) 11592, https://doi.org/10.3390/app112411592.
[4] G. Zhou, et al., The European DEMO helium cooled pebble bed breeding blanket: design status at the conclusion of the pre-concept design phase, Energies 16 (14) (2023) 5377, https://doi.org/10.3390/en16145377.
[5] P.A. Di Maio, et al., Thermofluid-dynamic and thermal–structural assessment of the EU-DEMO WCLL "double bundle" Breeding Blanket concept left outboard segment, Fusion Eng. Design 202 (2024) 114335, https://doi.org/10.1016/j.fusengdes.2024.114335. ISSN 0920-3796.
[6] S. Giambrone, et al., Preliminary thermo-mechanical assessment of the top cap region of the water-cooled lead-ceramic breeder breeding blanket alternative concept, Fusion Eng. Design 200 (2024) 114201, https://doi.org/10.1016/j.fusengdes.2024.114201. ISSN 0920-3796.
[7] R. Gaisin, Progress in Manufacture, Processing and Characterization of NMM –2022, EUROfusion IDM Ref.: 2Q7T4P, 2022.
[8] Hernández F.A. et al., "Innovative breeding blanket concepts and overview of future R&D needs for breeding blanket development in the EU, Workshop On Advancements in Fusion Breeding Blankets Development, November 5-6, 2024, Hefei, China".
[9] G. Zhou, et al., HCPB Design and Analysis – Interim Report 2022, EUROfusion IDM Ref.: 2Q4YMC v1.0, 2019.
[10] G. Veres, et al., Thermo-Hydraulic Analysis Support –2018, EUROfusion IDM Ref.: 2P3AQ7 v1.0, 2019.
[11] G. Zhou, File "Nuclear_heat_SP9-npd-D_March2023.xlsx, 2023 personal communication.
[12] I.A. Maione, et al., BB HCPB System Requirements Document (SRD) For the Definition Dossier, EUROfusion IDM Ref.: 2PAUZ4 v1.5, 2020.